Catalysts **2015**, *5*, 1704-1720; doi:10.3390/catal5041704

OPEN ACCESS

catalysts

ISSN 2073-4344

www.mdpi.com/journal/catalysts

Article

VO_x Surface Coverage Optimization of V_2O_5/WO_3-TiO_2 SCR Catalysts by Variation of the V Loading and by Aging

Adrian Marberger [1,2], Martin Elsener [1], Davide Ferri [1] and Oliver Kröcher [1,2,*]

[1] Paul Scherrer Institut, CH-5232 Villigen, Switzerland; E-Mails: adrian.marberger@psi.ch (A.M.); Martin.Elsener@psi.ch (M.E.); davide.ferri@psi.ch (D.F.)

[2] Ecole polytechnique fédérale de Lausanne (EPFL), CH-1015 Lausanne, Switzerland

***** Author to whom correspondence should be addressed; E-Mail: oliver.kroecher@psi.ch; Tel.: +41-56-310-20-66.

Academic Editor: Jae-Soon Choi

Received: 24 August 2015 / Accepted: 1 October 2015 / Published: 14 October 2015

Abstract: V_2O_5/WO_3-TiO_2 selective catalytic reduction (SCR) catalysts with a V_2O_5 loading of 1.7, 2.0, 2.3, 2.6, 2.9, 3.2 and 3.5 wt. % were investigated in the fresh state and after hydrothermal aging at 600 °C for 16 h. The catalysts were characterized by means of nitrogen physisorption, X-ray diffraction and X-ray absorption spectroscopy. In the fresh state, the SCR activity increased with increasing V loading. Upon aging, the catalysts with up to 2.3 wt. % V_2O_5 exhibited higher NO_x reduction activity than in the fresh state, while the catalysts with more than 2.6 wt. % V_2O_5 showed increasing deactivation tendencies. The observed activation and deactivation were correlated with the change of the VO_x and WO_x surface coverages. Only catalysts with a VO_x coverage below 50% in the aged state did not show deactivation tendencies. With respect to tungsten, above one monolayer of WO_x, WO_3 particles were formed leading to loss of surface acidity, sintering, catalyst deactivation and early NH_3 slip. An optimal compromise between activity and hydrothermal aging resistance could be obtained only with V_2O_5 between 2.0 and 2.6 wt. %.

Keywords: SCR; V_2O_5; surface coverage; V loading; hydrothermal aging; WO_3-TiO_2

---

1. Introduction

Vanadium containing catalysts are used worldwide as efficient post-treatment catalysts for reducing nitrogen oxides emissions in stationary applications. In this process, NO_x reacts with injected NH_3 (selective catalytic reduction (SCR)) according to Equation (1) [1].

$$4NO + 4NH_3 + O_2 = 4N_2 + 6H_2O \quad (1)$$

Since 2005, V-based SCR catalysts have also been applied in mobile sources such as heavy-duty Diesel vehicles, where a urea solution is used as a non-poisonous NH_3 source [2]. With the most recent NO_x emission regulations such as the Euro 6 standards, NH_3-SCR becomes a promising technology also for light-duty Diesel engines.

The SCR catalyst typically consists of anatase TiO_2 as support material, WO_3 as a promoter for activity and stability and around 2 wt. % V_2O_5 as the active redox species [3–5]. Despite the conventional V_2O_5 notation, vanadium is actually dispersed as VO_x species over the high surface area support [6–8]. WO_3 is proposed to have multiple promoting effects including the prevention of V island formation [7], increase the number of NH_3 adsorption sites [9] or improvement of thermal stability of the thermodynamically unfavorable anatase phase [4]. Extensive research has been undertaken to understand the different aspects of standard V-based SCR catalysts. These efforts were aimed at revealing mechanistic details such as the nature of the active centers and the rate determining steps [10–17], the origin of catalyst aging [18] and the electronic interactions between the various catalyst components and the poisoning phenomena [19–21]. For this purpose, parameters such as the synthesis of the TiO_2 support material [22,23], the synthesis method, the loading and the nature of WO_3 and V_2O_5 and the structural change upon thermal/hydrothermal treatment have been addressed.

The V content on a WO_3-TiO_2 (WT) support is a crucial aspect for the activity and stability of the catalyst. A low V_2O_5 content of 0.5–1.5 wt. % is often chosen for stationary applications, where the volume of the catalytic converter and the activity are not key properties. Instead, sulfur resistance, longevity and production costs are of higher significance [24]. In mobile sources, V-based catalysts need to be highly active due to the limited available space for the exhaust gas treatment system. Hence, the V_2O_5 content is increased to 2–3 wt. %. Moreover, these catalysts have to operate in a broader temperature window ranging from cold start conditions to full engine load [25]. Finally, the SCR catalyst may experience severe temperature surges because of the regeneration of the upstream diesel particulate filter.

The V loading has been investigated on various support materials such as Al_2O_3, ZrO_2, SiO_2 or TiO_2 [3,7,26–28]. Among these, WT has often been used for V-based SCR catalyst preparation. Madia *et al.* examined the thermal stability of 1, 2 and 3 wt. % V_2O_5/WT [18]. The most active and thermally stable catalyst at 600 °C was found at 2 wt. % V_2O_5. The structural investigation revealed that the enhanced SCR performance is related to the amount of polymeric vanadyl surface species generated by the thermal aging. The decrease in the SCR performance for the high V-loaded catalyst upon aging was related to the loss of surface area and to the growth of three-dimensional vanadia species. Went *et al.* [26] investigated the different V species by varying the V_2O_5 loading on TiO_2 from 1.3 wt. % to, 2.5, 3.0, 6.1 and 9.8 wt. %. It was shown that both monomeric and polymeric VO_x species are present up to 3 wt. % V_2O_5, while crystalline V_2O_5 was only detected above 6 wt. % V_2O_5.

Lee *et al.* [29] investigated V_2O_5/WT with a V_2O_5 loading of 1, 3, 5, 7 and 10 wt. % and different preparation methods. The 3 wt. % V_2O_5/WT exhibited the highest NO_x reduction activity in the fresh state at 450 °C and after aging at 650 °C. The V loading of V_2O_5/WT has been the object of attention of other authors as well, e.g. Putluru *et al.* [30] (1.5 and 3.0 wt. % V_2O_5/WT), Amiridis *et al.* [31] (1.0, 2.0, 3.5, 3.9, 6.6, 8.5, 11.1, and 15.9 wt. % V_2O_5/WT), Kompio *et al.* [7] (0.5, 1.5, 3.0, 5.0 wt. % V_2O_5/WT) and Djerad *et al.* [3] (3 and 8 wt. % V_2O_5/WT). All these studies emphasize the importance of an optimal V loading on a TiO_2-based SCR catalyst. However, the adjustment of the loading only slightly around 2–3 wt. % V_2O_5, the concentration range relevant for real-world applications, is missing.

The calcination and aging of V_2O_5/WT catalysts cause a change of the surface area that is directly linked to the surface density of vanadyl species and as a consequence also the catalytic performance. As Kwon *et al.* [32] pointed out, one can determine the optimal surface density of the vanadyl species that is crucial for a high catalytic activity. By variation of the V loading (0, 0.5, 1.0, 1.5 and 2.0 wt. % V_2O_5) in V_2O_5/TiO_2 catalysts, a VO_x surface density of 4.5 VO_x nm^{-2} was found to be optimal for high NO_x reduction activity. This corresponds to a surface coverage of 55–60%, based on the theoretical maximum VO_x surface density of 7.9 VO_x nm^{-2} [33].

In this study, the V_2O_5 loading of a V_2O_5/WT catalyst was fine-tuned and the importance of this parameter for the optimum performance of the catalyst is demonstrated. The catalyst composition was systematically altered by loading a WT support with 1.7, 2.0, 2.3, 2.6, 2.9, 3.2 and 3.5 wt. % V_2O_5. Additionally, the catalysts were hydrothermally aged in order to mimic long-term use. The aging influenced the surface area of the catalyst, which consequently altered the VO_x surface coverage and the catalytic activity. It is shown that a subtle variation of the V content around the optimum value causes severe changes in the aging characteristics of V_2O_5/WT catalysts.

2. Results and Discussion

2.1. Catalytic Activity

The NO_x reduction activity of fresh and the hydrothermally aged V_2O_5/WO_3-TiO_2 (V_2O_5/WT) catalysts with increasing V_2O_5 is reported in Figures 1a and 1b, respectively. Since hydrothermal aging is more practice-relevant compared to thermal aging, the washcoated monoliths were aged at 600 °C for 16 h (GHSV = 10,000 h^{-1}) under a continuous flow of 5 vol. % O_2 and 10 vol. % H_2O in a flow reactor. All curves in Figure 1a are characterized by a steep increase in activity between 200 °C and 300 °C. In the 350–450 °C temperature regime, the catalysts exhibited an efficiency that was often higher than 95%. Between 500 °C and 550 °C, the NO_x reduction activity always decreased due to a selectivity loss (NH_3 oxidation to N_2 or NO).

Below 300 °C, the fresh catalysts showed increasing NO_x reduction activity under NH_3 excess (maximum $DeNO_x$) with increasing V_2O_5 loading from 1.7 wt. % to 3.5 wt. %. The NO_x reduction activity values measured at 250 °C are reported in Table 1 for comparison. As an example, the maximum NO_x reduction activity for 2.0 wt. % V_2O_5 at 250 °C and 300 °C was 37% and 78%, respectively, while it was 75% (250 °C) and 96% (300 °C) for the highest loading of 3.5 wt. %. At 550 °C, the trend was reversed and high loading was no longer beneficial for a high NO_x reduction activity. The catalyst with 3.5 wt. % V_2O_5 showed severe selectivity losses so that the originally broad operation window shrank

significantly. In the ideal temperature regime of 350–450 °C, all catalysts had NO_x reduction activities higher than 95 %.

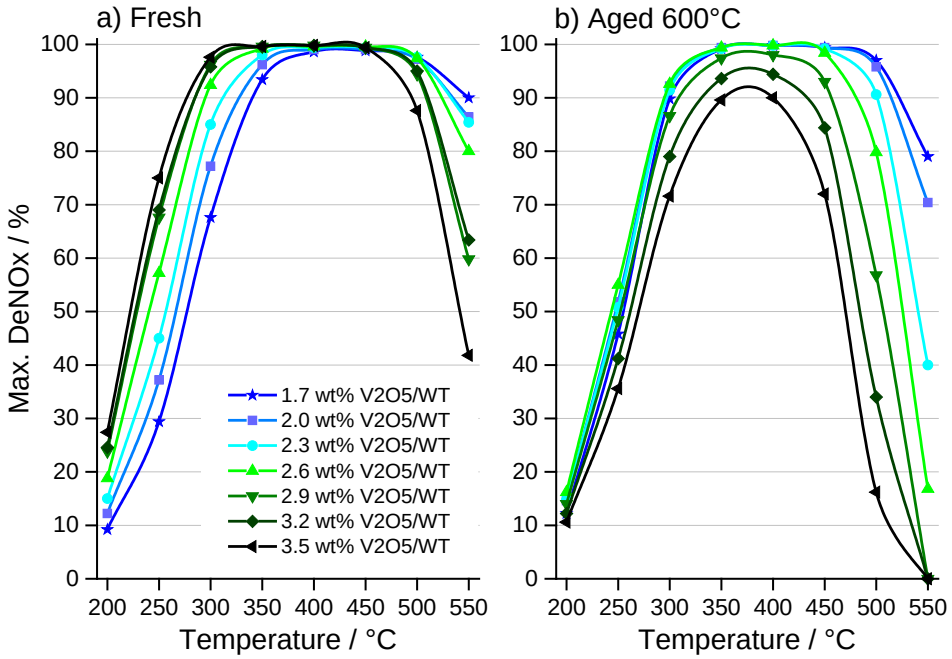

Figure 1. NO_x reduction activity under NH_3 excess (maximum $DeNO_x$) of 1.7–3.5 wt. % V_2O_5/WT (**a**) in the fresh state and (**b**) in the aged state (hydrothermal aging at 600 °C for 16 h).

The aged catalysts (Figure 1b) showed deactivation tendencies for high V_2O_5 loading. Below 300 °C, the catalysts with a loading up to 2.3 wt. % V_2O_5 benefited from the aging and became more active than in the fresh state. This was especially evident for the samples with 2.0 and 2.3 wt. % V_2O_5, whose NO_x reduction activities were higher than 50% at 250 °C and 90% at 300 °C, respectively (Table 1). While for 2.6 wt. % V_2O_5, the NO_x reduction activity was comparable to that in the fresh state, the deactivation was more pronounced at higher loadings.

Table 1. NO_x reduction activity (%) at 250 °C for the fresh and the aged catalysts as function of V_2O_5 loading. Data are from Figure 1.

V_2O_5 (wt. %)	**1.7**	**2.0**	**2.3**	**2.6**	**2.9**	**3.2**	**3.5**
fresh	29.4	37.2	45.0	57.2	67.6	69.0	75.0
aged	45.8	51.8	50.8	55.0	48.4	41.2	35.6

In the medium temperature regime, the catalysts with a loading higher than 2.6 wt. % V_2O_5 suffered from deactivation. In the high temperature regime, the NO_x reduction activity was below 60% for catalysts with more than 2.6 wt. % V_2O_5. It is important to mention that the entire temperature range of 200–550 °C is required for a complete performance test. If the catalysts are tested only up to 450 or 500 °C, the negative effect of a high V content cannot be perceived. The hydrothermal aging at 600 °C is not very severe but high enough to reveal that the V_2O_5 loading on WT should not exceed 2.6 wt. % to guarantee sufficient catalyst stability. Below 2.0 wt. % V_2O_5/WT, the aging did not affect the catalyst negatively but on the other side the activity in the low temperature regime was too low for these catalysts.

A good compromise between low temperature activity, stability and high temperature selectivity was found for a loading between 2.0 and 2.6 wt. % V_2O_5 on WT.

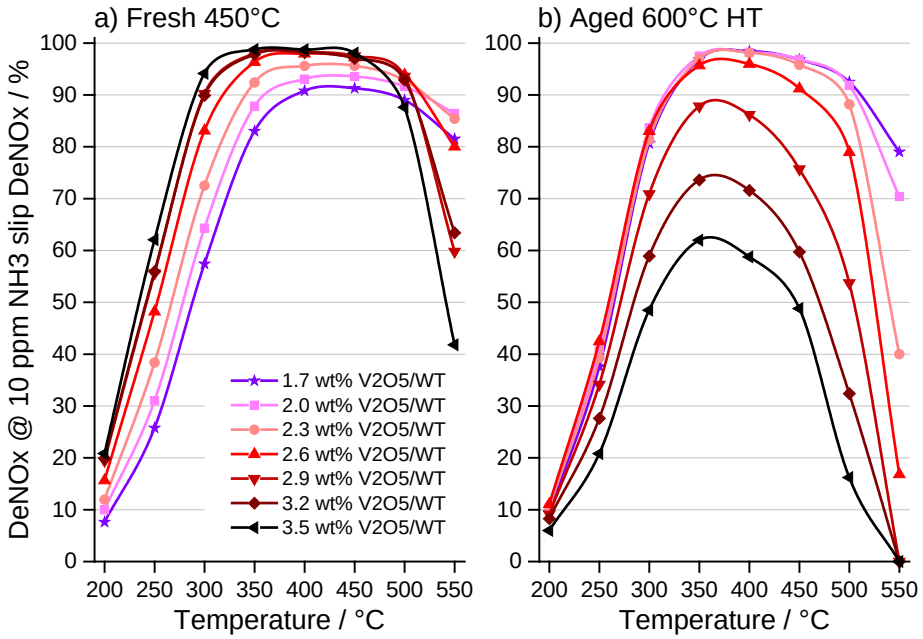

Figure 2. NO_x reduction activity ($DeNO_x$) at 10 ppm NH_3 slip of 1.7–3.5 wt. % V_2O_5/WT (**a**) in the fresh state and (**b**) in the aged state (hydrothermal aging at 600 °C for 16 h).

Similar trends to the maximum $DeNO_x$ of Figure 1 are observed for the $DeNO_x$ at 10 ppm NH_3 slip, which is shown in Figure 2. The main difference is that the effect of loading and aging were more pronounced. With a maximum permissible NH_3 slip of 10 ppm, which is relevant for practical applications, often lower NO_x conversions are obtained than for equimolar dosing conditions or for excess NH_3 dosage [1,25,34,35].

While a high V loading was advantageous for high NO_x reduction activity in the fresh state (Figure 2a), a low loading was beneficial after aging of the catalyst (Figure 2b). The catalysts with low V loading exhibited an activation, *i.e.* an improved NO_x reduction activity compared to the fresh state. An additional feature of the highly V-loaded catalysts in the fresh state is the late NH_3 slip during $DeNO_x$ at 10 ppm NH_3 slip. This is observable by comparing, e.g., 3.2 wt. % V_2O_5 in Figure 2a and Figure 1a. The catalyst exhibited similar NO_x reduction activities, evidencing that the NH_3 slip is not critical; in the aged state, however, the NH_3 slip was more pronounced for higher V_2O_5 loadings. Hence, the difference between maximum $DeNO_x$ and $DeNO_x$ at 10 ppm NH_3 slip became larger. Therefore, the impact of aging can be better evaluated when the $DeNO_x$ at 10 ppm NH_3 slip is considered. The reason for the enhanced significance of the deactivation is likely related to the fact that the surface acidity is indirectly included in the information delivered by the NH_3 slip measurement. If a catalyst loses surface acidity, e.g. by sintering of WO_3, the NH_3 uptake decreases while the NH_3 slip increases. Therefore, the deactivation of high V-loaded catalysts in the aged state (Figure 2b) demonstrates that these catalysts possess lower surface acidity compared to the fresh catalysts.

In the low temperature regime of 200–300 °C, where NO_x conversion is determined by the catalyst activity and mass transfer limitations are negligible [25,36,37], the reaction rate constant k_{mass}

(Figure 3) was calculated according to Equation (2). With this value, the catalysts can be compared irrespective of the small loading deviations of the washcoat.

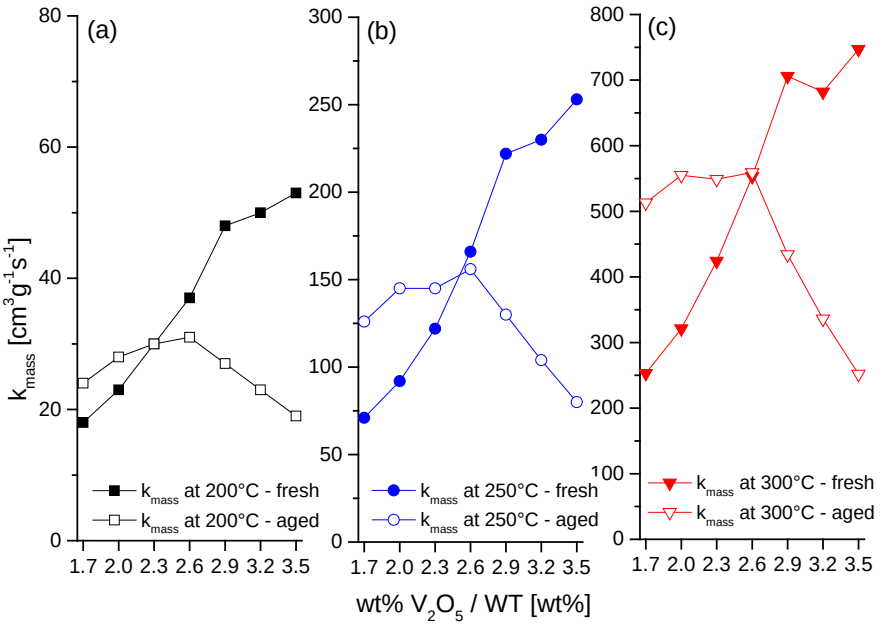

Figure 3. Reaction rate constant k_{mass} determined at (**a**) 200 °C, (**b**) 250 °C and (**c**) 300 °C as a function of V_2O_5 loading in the fresh and the aged state.

It is evident that k_{mass} of the fresh catalysts increased from 1.7 to 2.9 wt. % V_2O_5, whereas it only slightly increased from 2.9 to 3.5 wt. % V_2O_5. This behaviour is common to all temperatures in Figure 3a–c. A higher loading than 2.9 wt. % V_2O_5 was therefore no longer beneficial for catalysts in the fresh state. In the aged state, the catalysts with 2.0–2.6 wt. % V_2O_5 exhibited a k_{mass} of around 30, 150 and 550 $cm^3g^{-1}s^{-1}$ at 200, 250 and 300 °C, respectively. At the lowest loading of 1.7 wt. % V_2O_5, k_{mass} was lower compared to the loadings around 2.3 wt. % V_2O_5. At higher loading than 2.6 wt. % V_2O_5, k_{mass} linearly decreased to about half of the maximum rate constant for 2.6 wt. % V_2O_5/WT. By comparing the fresh and the aged catalysts, it is apparent that they were only deactivated above 2.6 wt. % V_2O_5. For 1.7–2.0 wt. % V_2O_5, k_{mass} increased upon aging, while no effect of aging was observed for loadings between 2.3 and 2.6 wt. % V_2O_5.

The performance tests in the fresh and the aged state clearly indicate that the V_2O_5 loading should be adjusted between 2.0 and 2.6 wt. % for a WO_3/TiO_2 support material. Only in this range, a compromise between good activity and hydrothermal aging resistance was obtained. The determination of the $DeNO_x$ at 10 ppm NH_3 slip is an important performance test, which reveals the deactivation effect more markedly than the measurement of the maximum $DeNO_x$.

2.2. Characterization

The washcoat material remaining from the slurries was dried and calcined at 550, 600, 650 and 700 °C for 10 h and analyzed using nitrogen physisorption (BET method), X-ray diffraction (XRD) and X-ray absorption near edge spectroscopy (XANES).

The change of the BET specific surface area (SSA) of 2.0, 2.9 and 3.5 wt. % V_2O_5/WT upon calcination is displayed in Figure 4a. These three samples were chosen to adequately represent the V loading range. After calcination at 550 °C, the SSA of all V-loaded catalysts was lower (by *ca.* 15 m^2/g) than that of the WT support material irrespective of V_2O_5 loading. In contrast, by increasing the calcination temperature to 600 °C, it becomes evident that a high V loading negatively affected the SSA. For 2.0 wt. % V_2O_5/WT, the SSA decreased only by 5 m^2/g (−7%), while it decreased from 64 m^2/g to 38 m^2/g (−41%) for 3.5 wt. % V_2O_5/WT. The increase in calcination temperature from 600 °C to 650 °C had a similar effect on all catalysts, *i.e.* the SSA decreased by further 25 m^2/g. While 2.0 wt. % V_2O_5/WT still had a residual SSA of 35 m^2/g, the SSA of 3.5 wt. % V_2O_5/WT decreased to 13 m^2/g. At 700 °C, the loading did not play a role anymore and the SSA of all V_2O_5/WT was reduced to below 10 m^2/g. For a loading of 2.9 wt. % V_2O_5, the SSA linearly decreased by 15–20 m^2/g with each 50 °C increase in temperature. In contrast to the V-loaded samples, the support material WT exhibited a SSA of 44 m^2/g after calcination at 700 °C. This confirms the observation that vanadium assists the sintering of the support material [18]. It is also evident that a high vanadium content accelerates sintering, *i.e.* sintering can start already at lower calcination temperatures. The low melting point of V_2O_5 is typically considered responsible for the undesired effect of V on the dispersion of the W-containing phase [38].

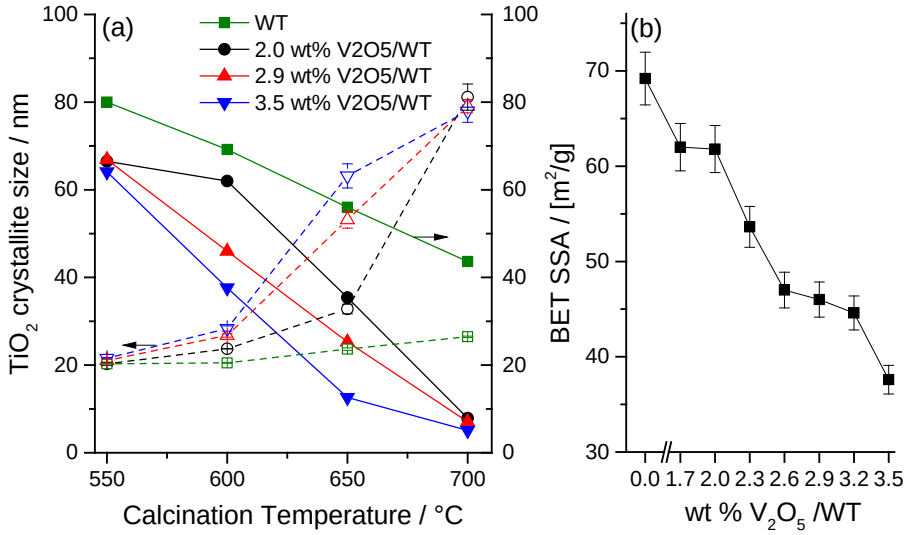

Figure 4. Calcination temperature dependence of (**a**) specific surface area (lines) and crystallite size (dashed lines) of WT, 2.0, 2.9 and 3.5 wt. % V_2O_5/WT. The crystallite size was obtained from the X-ray diffraction (XRD) reflections of anatase at 2Θ 25.4° and 48.0° using the Scherrer equation. (**b**) Specific surface area of all catalysts calcined at 600 °C.

The impact of loading on SSA is further demonstrated in Figure 4b, where the SSA of 1.7–3.5 wt. % V_2O_5/WT catalysts calcined at 600 °C is shown. The change of SSA between the support material WT and up to 2.0 wt. % V_2O_5 was below 10 m^2/g but decreased by about 5 m^2/g with every additional 0.3 wt. % V_2O_5. It should be noticed that by comparing maximum $DeNO_x$ and SSA at 600 °C, only loadings of 2.0 and 2.3 wt. % V_2O_5/WT seem to be optimal. Both samples have a SSA above 50 m^2/g and their activity/selectivity did not decrease upon aging.

The XRD patterns of 2.0, 3.5 wt. % V_2O_5/WT and WT are shown for various calcination temperatures in Figure 5a–c. Figure 6 further displays the patterns of all catalysts calcined at 600 °C with an additional inset for the WO_3 reflection at 2Θ 23.5°. In all diffractograms, the anatase peaks are visible at 2Θ 25.4° and between 37 and 40°.

For 2.0 wt. % V_2O_5 (Figure 5a), calcination up to 600 °C did not cause formation of any other XRD visible phase. Hence, we can assume that the vanadium and tungsten species are well dispersed or that their crystallite size is below the detection limit of XRD. At 650 °C, WO_3 was detected, which became more prominent at 700 °C together with the beginning of the anatase to rutile phase transformation. The crystallinity of the anatase phase visibly increased (2Θ 37.8°) with increasing calcination temperature.

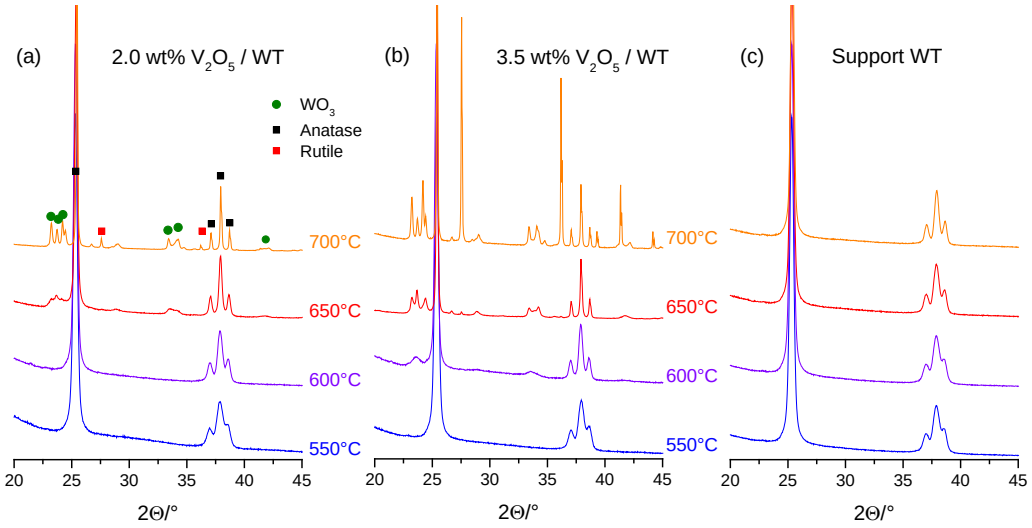

Figure 5. XRD patterns of (**a**) 2.0 wt. % V_2O_5/WT, (**b**) 3.5 wt. % V_2O_5/WT, and (**c**) WT calcined at the indicated temperatures. All diffractograms are normalized using the anatase peak at 2Θ 25.4°.

The XRD patterns of 3.5 wt. % V_2O_5/WT in Figure 5b revealed the same phase evolution as in Figure 5a. However, phase changes occurred already at lower calcination temperatures than in the case of 2.0 wt. % V_2O_5/WT. The WO_3 crystallites were already detected at 600 °C and the anatase to rutile phase transformation started at 650 °C. Despite structural changes, no V-containing phase was detected and the VO_x species seemed to remain well dispersed. The changes in the speciation of the WO_3 phase are associated with the presence of V in agreement with the BET observations (Figure 4). At identical calcination temperatures, WT did not present any evidence of WO_3 sintering.

The crystallite size of anatase TiO_2 was determined using the Scherrer equation from the XRD patterns of Figure 5 and the values are reported in Figure 4a. At 550 °C, the crystallite size was around 20 nm irrespective of the V loading. It increased already at 600 °C for catalysts with high V loading. At 650 °C, the deviation between low and high V loading was more pronounced and varied from 33 (±1) to 63 (±3) nm, respectively. At 700 °C, no significant size difference between low and high V loading was found (around 80 nm) in agreement with the similar SSA values. Both, the SSA and the crystallite size showed that the catalysts sintered with increasing V loading and increasing calcination temperature.

All catalysts were also analyzed by XRD after calcination at 600 °C (Figure 6). WO_3 was not visible below 2.3 wt. % V_2O_5 and the diffractograms approximately matched that of the support material, WT. The contribution of WO_3 appeared first for 2.6 wt. % V_2O_5/WT and became more prominent with increasing V loading.

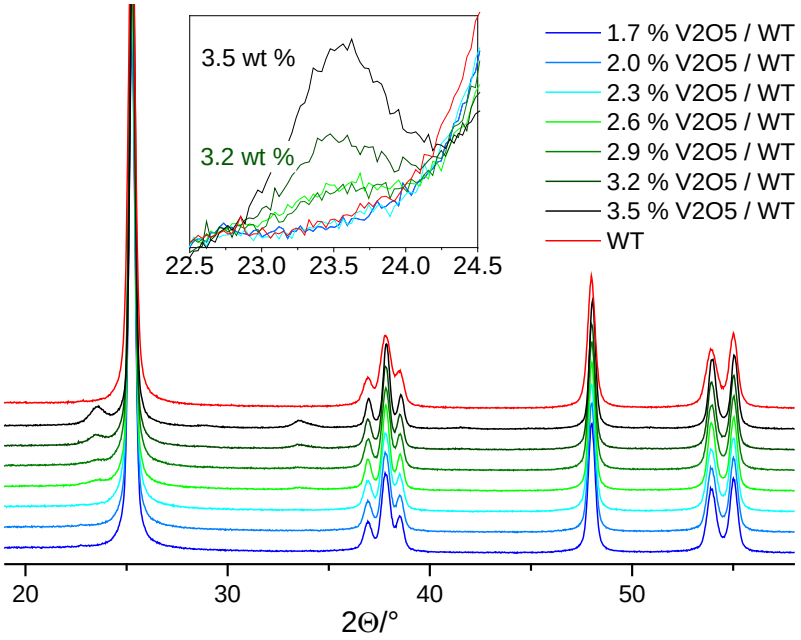

Figure 6. XRD patterns of 1.7–3.5 wt. % V_2O_5/WT calcined at 600 °C.The inset shows a magnification around the WO_3 peak at 2Θ 23.5°. All diffractograms are normalized using the anatase peak at 2Θ 25.4°.

Since XRD was not able to provide information on V because of its low loading and low aggregation state, two catalysts were selected for an element specific characterization. The local environment of the VO_x species supported on WT was studied using X-ray absorption near edge structure spectroscopy (XANES).

The normalized XANES spectra of 2.0 and 3.5 wt. % V_2O_5 /WT calcined at 550 and 650 °C recorded at the V K-edge are shown in Figure 7. Without attempting a quantitative assessment of both oxidation state and coordination of the VO_x species represented by these spectra, a qualitative discussion is sufficient to support our interpretation of the loading and sintering effects. The spectra of 2.0 and 3.5 wt. % V_2O_5/WT calcined at 550 °C are comparable, suggesting a similar local environment of V. This is in agreement with the XRD data of Figure 5, where no formation of any VO_x phase was observed because the agglomerates were not crystalline enough or below the detection limit. Upon calcination at 650 °C, an obvious change in the XANES region is observed for 3.5 wt. % V_2O_5/WT. The whiteline region (up to 5.52 keV) develops three features characteristic of V_2O_5, suggesting that the VO_x species evolved to form V_2O_5-like agglomerates [2,25]. This change is correlated with the increase of VO_x surface coverage from 46% in 2.0 wt. % V_2O_5/WT to 232% in 3.5 wt. % V_2O_5/WT that is discussed in the next section. Hence, VO_x started to adopt a different local environment when the VO_x surface coverage exceeded one theoretical monolayer.

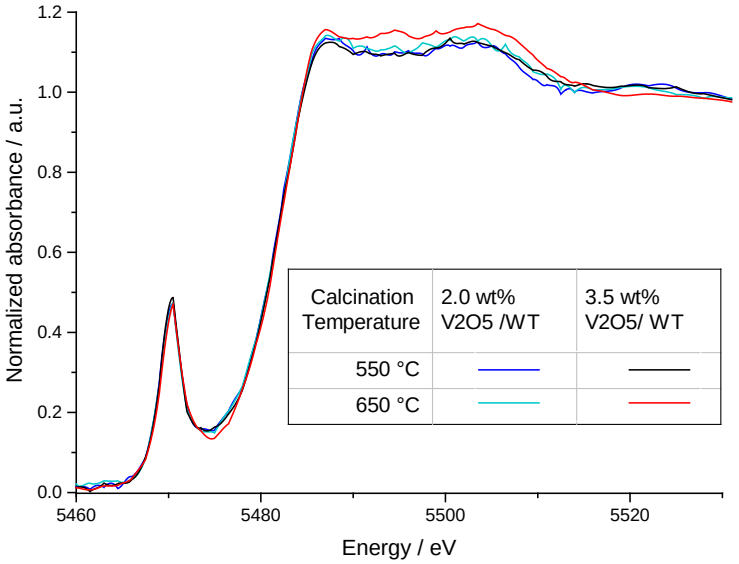

Figure 7. Normalized V K-edge X-ray absorption near edge structure spectroscopy (XANES) spectra of selected catalysts in the fresh and the aged state.

2.2.1. VO_x Surface Coverage

The surface coverage of VO_x and WO_x provides additional insight for structure–activity relationships. The VO_x and WO_x surface coverages were calculated from the SSA considering that the theoretical saturation values for the monolayer coverage are 7.9 VO_x nm^{-2} and 4.2 WO_x nm^{-2}, respectively [33]. As a result, Figure 8 shows the surface coverage of a low, medium and high loaded V_2O_5/WT catalyst at various calcination temperatures.

For both high SCR activity and selectivity, the VO_x coverage should be below the monolayer level [30]. The VO_x coverage in Figure 8a was below 50% for a calcination at 550 °C and below 100% for all catalysts at 600 °C. At 650 °C, 3.5 wt. % V_2O_5/WT exceeds the monolayer coverage and at 700 °C, all catalysts theoretically exhibit a multilayer of VO_x species. This was not observable by XRD (Figure 5) but only in the XANES spectra (Figure 7), which revealed polymeric VO_x with a vanadium environment similar to that of V_2O_5.

Figure 8c further displays the VO_x coverage of all catalysts calcined at 600 °C, which varies from 24% to 78%. This corresponds well with the XRD observation and the absence of V_2O_5. A vanadium coverage of around 27, 36 and 46% was calculated for 2.0, 2.3 and 2.6 wt. % V_2O_5/WT calcined at 600 °C, respectively. By comparing the VO_x coverage with the rate constants in Figure 3a–c, it can be concluded that an optimized VO_x coverage should be between 25–50%. Below this value, the catalysts seem to have not enough active sites for the SCR reaction, while above 50%, the catalysts showed strong selectivity issues. This is evident from Figure 8a. The fresh 3.5 wt. % V_2O_5/WT catalyst had a surface coverage of 46% and was very active. Upon aging at 600 °C, the coverage increased to 78% and the catalyst experienced strong deactivation. Similar considerations apply for the activation of catalysts with a low V loading. After increasing the calcination from 550 to 650 °C, the VO_x coverage of, e.g., 2.0 wt. % V_2O_5/WT increased from below 25% to roughly 50% (Figure 8a), which is a plausible explanation for the activation.

A study by Amiridis *et al.* [31] estimated an optimum V_2O_5 coverage of around 2 µmol/m^2 (2.4 VO_x/nm^2 = 30% surface coverage) for V_2O_5/TiO_2 doped with around 0.8 wt. % WO_3. The optimum catalyst was chosen from the activation energy of the catalysts, which only slightly decreased with further increasing the V content. Kwon *et al.* [32] have shown that VO_x coverage of 55–60% is optimal for the catalytic activity of V_2O_5/TiO_2. In the present system, the optimum coverage seems to be lower, which can be explained by the enhanced surface acidity induced by WO_3 [4]. Adsorbed NH_3 becomes more readily available for the SCR reaction; hence a lower VO_x coverage is sufficient for optimizing the catalyst performance in the presence of WO_3.

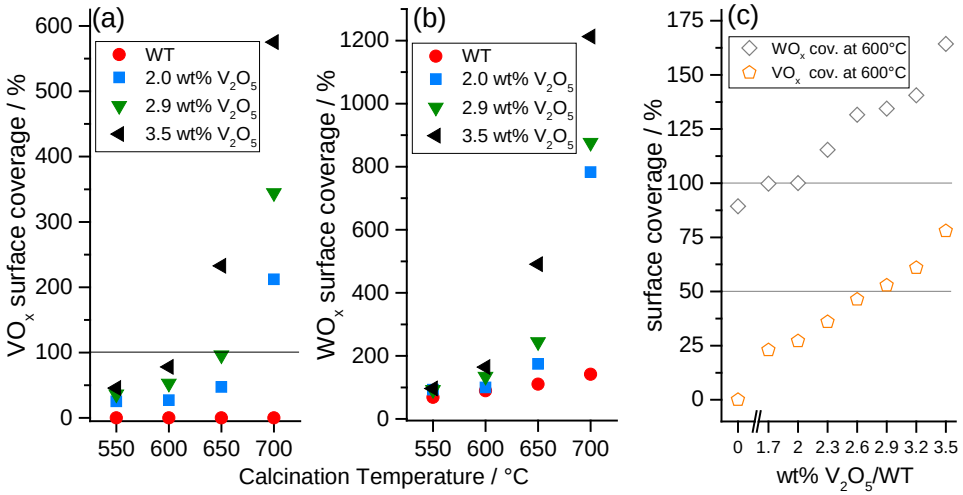

Figure 8. Surface coverage of (**a**) VO_x and (**b**) WO_x for the support material WT and three different catalysts as function of calcination temperature. (**c**) Surface coverage of VO_x and WO_x as function of V_2O_5 loading at 600 °C.

2.2.2. WO_x Surface Coverage

In the case of WO_x (Figure 8b), only calcination at 550 °C produced a sub-monolayer coverage for all catalysts. Already at 600 °C, the catalysts with high V content exceeded the theoretical WO_x monolayer as shown in greater detail in Figure 8c. Up to 2.0 wt. % V_2O_5, the WO_x coverage remained below one monolayer, while it was slightly above for 2.3 wt. % V_2O_5 (115%). For higher V contents, the WO_x surface coverage increased in agreement with the XRD observation of Figure 6. At 2.6 wt. % V_2O_5 or higher, WO_3 crystallites were detected and the WO_x surface coverage was noticeably above one monolayer.

Comparison of the surface coverage with the NO_x reduction performance in Figures 1b and 2b suggests that the aging at 600 °C and catalyst activation/deactivation can be correlated with the increase in surface coverage of WO_x. Tungsten oxide provides acid sites to the catalyst where the NH_3 is supposed to adsorb and be readily available for the SCR reaction [4]. Upon calcination at increasing temperature, the fraction of available WO_x species and hence the surface acidity decrease and the catalyst increasingly loses activity. This is clearly visible from the DeNO$_x$ at 10 ppm NH_3 slip (Figure 2). The decrease in acidity caused by crystallization of WO_3 reduces the potential adsorption sites for NH_3 thus enhancing the 10 ppm NH_3 slip.

3. Experimental Section

3.1. Materials

All samples were prepared by wet impregnation of a commercial WO_3/TiO_2 (WT) support with NH_4VO_3. NH_4VO_3 (equivalent (eq.) to 1.7–3.5 wt. % V_2O_5, Sigma Aldrich, Buchs, Switzerland,) was dissolved in H_2O (10 mL) and added to a 30 mL aqueous slurry of WO_3/TiO_2 (WT, 12 g, "Tiona DT-52", 10 wt. % WO_3 and 90 wt. % TiO_2, Cristal Global, Thann, France). After the slurry was sonicated for 10 min in an ultrasonic bath, homogenized with a disperser (Miccra D-8, Schmizo AG, Zofingen, Switzerland, 20,000 rpm, 5 min) and stirred for 60 min, water was evaporated under reduced pressure and the sample was dried at 120 °C for 12 h. Finally, the sample was grinded thoroughly and was calcined at 550 °C in a muffle oven for 5 h (fresh catalyst).

For washcoating, the powders were suspended in a mixture of water (2 eq. of sample) and colloidal silicate (Ludox, 40 wt. % in H_2O, Sigma Aldrich, 0.1 eq. of TiO_2). After sonication of the slurry for 10 min in an ultrasonic bath, the honeycomb monoliths (cordierite, 400 cpsi, *ca*. 12 × 17 × 50 mm) were dip coated. The monoliths were repeatedly immersed in the slurry and dried with an air blower to reach a loading of the active material of around 1.25–1.35 g. The monoliths and the remaining slurry were dried overnight at 120 °C and calcined at 450 °C for 10 h in a muffle oven. The hydrothermal aging of the washcoated monoliths (600 °C for 16 h) was performed in a lab scale flow reactor in 20 vol% O_2 and 10 vol% H_2O with balance N_2 at GHSV = 10,000 h^{-1}.

3.2. Catalytic Measurements

The washcoated monoliths were tested in a laboratory test reactor described elsewhere [34,39] under a feed of 10 vol% O_2, 5 vol% H_2O, 500 ppm NO, 0–600 ppm NH_3 with balance N_2, in order to mimic realistic exhaust gas composition. The gas hourly space velocity (GHSV = volumetric gas flow/coated monolith volume) was 50,000 h^{-1}, which is typical of SCR converters of diesel vehicles [39]. The maximum NO_x reduction activity was measured by dosing NH_3 in excess, *i.e.* at NH_3/NO_x = 1.2. The excess of NH_3 is exploited to achieve a maximum $DeNO_x$ that is not affected by possible side reactions of NH_3. Since equation 1 is in zeroth order with respect to NH_3, the NH_3 does not influence the equilibrium. In order to obtain a more practice-oriented value for SCR systems, the NO_x reduction activity at 10 ppm NH_3 slip was measured as well, as described earlier [1,25,34,35]. The mass specific rate constant (k_{mass}) for the maximum $DeNO_x$ was calculated according to Equation (2), under the assumption of a pseudo-first order of the SCR reaction with respect to NO and zeroth order with respect to NH_3 [40,41],

$$k_{mass} = -\frac{V^*}{W} \cdot \ln(1 - X_{NO_x}) \quad (2)$$

where V^* is the total flow rate at reaction condition, W the loading of the active component and X_{NOx} the fractional NO_x conversion. Although adsorption of both NH_3 and NO occurs at low temperature [1], NH_3 adsorption dominates on acidic SCR catalysts so that the first order SCR reaction with respect to NO is justified. The rate constant is independent of the active component loading, which is particularly important for coated monoliths where small loading deviations are unavoidable. The NO_x reduction efficiency ($DeNO_x$) was estimated according to Equation (3), [3,41],

$$\mathrm{DeNO}x = \frac{\mathrm{C}_{\mathrm{NO}}^{\mathrm{in}} - \mathrm{C}_{\mathrm{NO}_x}^{\mathrm{out}}}{\mathrm{C}_{\mathrm{NO}}^{\mathrm{in}}} \cdot 100\% \quad (3)$$

where C^{in}_{NO} is the NO concentration upstream of the catalyst and C^{out}_{NOx} the NO and NO_2 concentrations downstream of the catalyst. Online gas analysis of the exhaust gas was performed with a Fourier transform infrared spectrometer (Nexus 670 ThermoNicolet, ThermoFisher, Schwerte, Germany) equipped with a heated gas cell.

3.3. Characterization Methods

The BET specific surface area (SSA) was measured by N_2 adsorption at −196 °C on a Quantachrome Autosorb I instrument (Quantachrome Instruments, Boynton Beach, FL, USA). Prior to the measurement, the samples were outgassed at 350 °C for 10 h. Powder X-ray diffraction (PXRD) patterns were collected on a D8 ADVANCE (Bruker AXS GmbH, Karlsruhe, Germany) diffractometer using Cu $K\alpha_1$ radiation (λ = 1.5406 Å). Data were recorded from 10 to 65° 2Θ using a step size of 0.03°/1 s acquisition time. The phases were identified with the X'Pert HighScore Plus software (2.0a, PANalytical B.V., Almelo, Netherlands, 2004). The crystallite size of TiO_2 was determined by the Scherrer equation using the peaks at 25.4° and at 48.0°. X-ray absorption near edge structure (XANES) spectra were recorded at beamline SuperXAS of the Swiss Light Source (SLS, Villigen, Switzerland). The spectra were collected around the V K-edge (E_0 = 5.465 keV) in fluorescence mode using double Si(111) crystal monochromator and a 10 µm V foil to calibrate the monochromator position. Samples were diluted with cellulose and pressed into pellets. The data were aligned, background corrected, and normalized using Athena (IFFEFIT software package, 1.2.11d, Free Software Foundation, Boston, MA, USA, 2013) [42].

4. Conclusions

We studied the activity and stability of V_2O_5/WO_3-TiO_2 SCR catalysts by systematically altering the vanadium content. Only V_2O_5 loadings between 2.0 and 2.6 wt. % withstand a moderate hydrothermal aging at 600 °C for 16 h and are in fact activated upon aging. Below 2.0 wt. % V_2O_5, sufficient activity cannot be guaranteed, while above 2.6 wt. % V_2O_5 deactivation upon aging increasingly occurs. On the base of NO_x reduction activity at 10 ppm NH_3 slip, we could show that the aging at high V_2O_5 loading is in fact more severe than one could anticipate from a standard measurement of the SCR activity with equimolar dosage of NH_3 and NO_x. The early NH_3 slip is a practical and direct indicator of the loss of surface acidity caused by the sintering of WO_3, which is confirmed by the XRD data. In the case of VO_x species at the loadings studied in this work, XRD is not able to yield any information. The evolution from highly dispersed VO_x species to a polymeric VO_x environment similar to that of V_2O_5 upon aging of the catalyst with a high V loading was qualitatively captured by V K-edge XANES.

The catalytic performance was further correlated with the surface coverage of WO_x and VO_x. An optimum surface VO_x coverage between 25–50 % was estimated, which can be adjusted by either the V loading or the specific surface area (calcination temperature). For the WO_x surface coverage, it was shown that above one WO_x monolayer, WO_3 crystallites are formed, thus diminishing the NH_3 uptake and hence the activity of the catalyst. It can be concluded that a V_2O_5 loading not higher than 2.6 wt. % should be used in SCR catalysts composed of V_2O_5, 10 wt. % WO_3 and TiO_2 in order to maintain the activity and stability of the catalyst.

Acknowledgments

The authors gratefully acknowledge financial support by Treibacher Industrie AG and the SLS for beamtime allocation at beamline SuperXAS.

Author Contributions

The experimental work was conceived and designed by A.M., M.E. and D.F.; M.E. and A.M. performed the experiments; A.M., and O.K, analyzed the data; M.E. contributed reagents/materials/analysis tools; A.M., D.F and O.K. drafted the paper. The manuscript was amended through the comments of all authors. All authors have given approval for the final version of the manuscript.

Conflicts of Interest

The authors declare no conflict of interest.

References

1. Koebel, M.; Elsener, M.; Kleemann, M. Urea-SCR: A promising technique to reduce NO_x emissions from automotive diesel engines. *Catal. Today* **2000**, *59*, 335–345.
2. Beale, A.M.; Lezcano-Gonzalez, I.; Maunula, T.; Palgrave, R.G. Development and characterization of thermally stable supported V–W–TiO_2 catalysts for mobile NH_3-SCR applications. *Catal. Struct. React.* **2015**, *1*, 25–34.
3. Djerad, S.; Tifouti, L.; Crocoll, M.; Weisweiler, W. Effect of vanadia and tungsten loadings on the physical and chemical characteristics of V_2O_5-WO_3/TiO_2 catalysts. *J. Mol. Catal. A* **2004**, *208*, 257–265.
4. Forzatti, P. Present status and perspectives in de-NO_x SCR catalysis. *Appl. Catal. A* **2001**, *222*, 221–236.
5. Nova, I.; Tronconi, E. *Urea-SCR Technology for DeNO_x After Treatment of Diesel Exhausts*; Springer: New York, NY, USA, 2014; pp. 6, 25 and 68.
6. Fierro, J.L.G. *Metal Oxides: Chemistry and Applications*; CRC Press: Florida, FI, USA, 2005; pp. 8–20.
7. Kompio, P.G.W.A.; Brückner, A.; Hipler, F.; Auer, G.; Löffler, E.; Grünert, W. A new view on the relations between tungsten and vanadium in $V_2O_5WO_3$/TiO_2 catalysts for the selective reduction of NO with NH_3. *J. Catal.* **2012**, *286*, 237–247.
8. Wachs, I.E. Recent conceptual advances in the catalysis science of mixed metal oxide catalytic materials. *Catal. Today* **2005**, *100*, 79–94.
9. Amiridis, M.D.; Duevel, R.V.; Wachs, I.E. The effect of metal oxide additives on the activity of V_2O_5/TiO_2 catalysts for the selective catalytic reduction of nitric oxide by ammonia. *Appl. Catal. B* **1999**, *20*, 111–122.
10. Anstrom, M.; Topsøe, N.-Y.; Dumesic, J.A. Density functional theory studies of mechanistic aspects of the SCR reaction on vanadium oxide catalysts. *J. Catal.* **2003**, *213*, 115–125.

11. Gruber, M.; Hermann, K. Elementary steps of the catalytic NO_x reduction with NH_3: Cluster studies on reaction paths and energetics at vanadium oxide substrate. *J. Chem. Phys.* **2013**, *139*, 244701–244708.
12. Ramis, G.; Yi, L.; Busca, G. Ammonia activation over catalysts for the selective catalytic reduction of NO_x and the selective catalytic oxidation of NH_3. An FT-IR study. *Catal. Today* **1996**, *28*, 373–380.
13. Topsøe, N.-Y. Mechanism of the Selective Catalytic Reduction of Nitric Oxide by Ammonia Elucidated by in Situ On-Line Fourier Transform Infrared Spectroscopy. *Science* **1994**, *265*, 1217–1219.
14. Topsøe, N.Y.; Dumesic, J.A.; Topsøe, H. Vanadia-Titania Catalysts for Selective Catalytic Reduction of Nitric-Oxide by Ammonia: I.I. Studies of Active Sites and Formulation of Catalytic Cycles. *J. Catal.* **1995**, *151*, 241–252.
15. Tronconi, E.; Nova, I.; Ciardelli, C.; Chatterjee, D.; Weibel, M. Redox features in the catalytic mechanism of the "standard" and "fast" NH_3-SCR of NO_x over a V-based catalyst investigated by dynamic methods. *J. Catal.* **2007**, *245*, 1–10.
16. Vittadini, A.; Casarin, M.; Selloni, A. First Principles Studies of Vanadia-Titania Monolayer Catalysts: Mechanisms of NO Selective Reduction. *J. Phys. Chem. B* **2005**, *109*, 1652–1655.
17. Zheng, Y.; Jensen, A.D.; Johnsson, J.E.; Thøgersen, J.R. Deactivation of V_2O_5-WO_3-TiO_2 SCR catalyst at biomass fired power plants: Elucidation of mechanisms by lab- and pilot-scale experiments. *Appl. Catal. B* **2008**, *83*, 186–194.
18. Madia, G.; Elsener, M.; Koebel, M.; Raimondi, F.; Wokaun, A. Thermal stability of vanadia-tungsta-titania catalysts in the SCR process. *Appl. Catal. B* **2002**, *39*, 181–190.
19. Nicosia, D.; Elsener, M.; Kröcher, O.; Jansohn, P. Basic investigation of the chemical deactivation of V_2O_5/WO_3-TiO_2 SCR catalysts by potassium, calcium, and phosphate. *Top. Catal.* **2007**, *42–43*, 333–336.
20. Xie, X.; Lu, J.; Hums, E.; Huang, Q.; Lu, Z. Study on the Deactivation of V_2O_5-WO_3/TiO_2 Selective Catalytic Reduction Catalysts through Transient Kinetics. *Energy Fuels* **2015**, *29*, 3890–3896.
21. Kamata, H.; Takahashi, K.; Odenbrand, C.U. I. The role of K_2O in the selective reduction of NO with NH_3 over a $V_2O_5(WO_3)/TiO_2$ commercial selective catalytic reduction catalyst. *J. Mol. Catal. A* **1999**, *139*, 189–198.
22. Zhang, X.; Li, X.; Wu, J.; Yang, R.; Zhang, Z. Selective Catalytic Reduction of NO by Ammonia on V_2O_5/TiO_2 Catalyst Prepared by Sol-Gel Method. *Catal. Lett.* **2009**, *130*, 235–238.
23. Georgiadou, I.; Papadopoulou, C.; Matralis, H.K.; Voyiatzis, G.A.; Lycourghiotis, A.; Kordulis, C. Preparation, Characterization, and Catalytic Properties for the SCR of NO by NH_3 of V_2O_5/TiO_2 Catalysts Prepared by Equilibrium Deposition Filtration. *J. Phys. Chem. B* **1998**, *102*, 8459–8468.
24. Alemany, L.J.; Lietti, L.; Ferlazzo, N.; Forzatti, P.; Busca, G.; Giamello, E.; Bregani, F. Reactivity and Physicochemical Characterization of V_2O_5-WO_3/TiO_2 De-NO_x Catalysts. *J. Catal.* **1995**, *155*, 117–130.
25. Marberger, A.; Elsener, M.; Ferri, D.; Sagar, A.; Schermanz, K.; Kröcher, O. Generation of NH_3 Selective Catalytic Reduction Active Catalysts from Decomposition of Supported $FeVO_4$. *ACS Catal.* **2015**, 4180–4188.

26. Went, G.T.; Leu, L.-j.; Bell, A.T. Quantitative structural analysis of dispersed vanadia species in TiO_2(anatase)-supported V_2O_5. *J. Catal.* **1992**, *134*, 479–491.
27. Burkardt, A.; Weisweiler, W.; van den Tillaart, J.A. A.; Schäfer-Sindlinger, A.; Lox, E.S. Influence of the V_2O_5 Loading on the Structure and Activity of V_2O_5/TiO_2 SCR Catalysts for Vehicle Application. *Top. Catal.* **2001**, *16–17*, 369–375.
28. Briand, L.E.; Tkachenko, O.P.; Guraya, M.; Gao, X.; Wachs, I.E.; Grünert, W. Surface-Analytical Studies of Supported Vanadium Oxide Monolayer Catalysts. *J. Phys. Chem. B* **2004**, *108*, 4823–4830.
29. Lee, B.W.; Hyun, C.; Shin, D.W. Characterization and De-NO_x activity of binary V_2O_5/TiO_2 and WO_3/TiO_2, and ternary V_2O_5-WO_3/TiO_2 SCR catalysts. *J. Ceram. Process. Res.* **2007**, *8*, 203–207.
30. Putluru, S.; Schill, L.; Gardini, D.; Mossin, S.; Wagner, J.; Jensen, A.; Fehrmann, R. Superior DeNO_x activity of V_2O_5-WO_3/TiO_2 catalysts prepared by deposition–precipitation method. *J. Mater. Sci.* **2014**, *49*, 2705–2713.
31. Amiridis, M.D.; Solar, J.P. Selective Catalytic Reduction of Nitric Oxide by Ammonia over V_2O_5/TiO_2, $V_2O_5/TiO_2/SiO_2$, and V_2O_5-WO_3/TiO_2 Catalysts: Effect of Vanadia Content on the Activation Energy. *Ind. Eng. Chem. Res.* **1996**, *35*, 978–981.
32. Kwon, D.W.; Park, K.H.; Hong, S.C. Influence of VO_x surface density and vanadyl species on the selective catalytic reduction of NO by NH_3 over VO*x*/TiO_2 for superior catalytic activity. *Appl. Catal. A* **2015**, *499*, 1–12.
33. Wachs, I.E. Raman and IR studies of surface metal oxide species on oxide supports: Supported metal oxide catalysts. *Catal. Today* **1996**, *27*, 437–455.
34. Kleemann, M.; Elsener, M.; Koebel, M.; Wokaun, A. Investigation of the ammonia adsorption on monolithic SCR catalysts by transient response analysis. *Appl. Catal. B* **2000**, *27*, 231–242.
35. Zhao, Y.; Hu, J.; Hua, L.; Shuai, S.; Wang, J. Ammonia Storage and Slip in a Urea Selective Catalytic Reduction Catalyst under Steady and Transient Conditions. *Ind. Eng. Chem. Res.* **2011**, *50*, 11863–11871.
36. Metkar, P.S.; Balakotaiah, V.; Harold, M.P. Experimental and kinetic modeling study of NO oxidation: Comparison of Fe and Cu-zeolite catalysts. *Catal. Today* **2012**, *184*, 115–128.
37. Koebel, M.; Madia, G.; Elsener, M. Selective catalytic reduction of NO and NO_2 at low temperatures. *Catal. Today* **2002**, *73*, 239–247.
38. Carreon, M.A.; Guliants, V.V. Ordered Meso- and Macroporous Binary and Mixed Metal Oxides. *Eur. J. Inorg. Chem.* **2005**, *2005*, 27–43.
39. Kröcher, O.; Devadas, M.; Elsener, M.; Wokaun, A.; Söger, N.; Pfeifer, M.; Demel, Y.; Mussmann, L. Investigation of the selective catalytic reduction of NO by NH_3 on Fe-ZSM5 monolith catalysts. *Appl. Catal. B* **2006**, *66*, 208–216.
40. Koebel, M.; Elsener, M. Selective catalytic reduction of NO over commercial DeNO_x-catalysts: experimental determination of kinetic and thermodynamic parameters. *Chem. Eng. Sci.* **1998**, *53*, 657–669.
41. Casapu, M.; Kröcher, O.; Elsener, M. Screening of doped MnO_x-CeO_2 catalysts for low-temperature NO-SCR. *Appl. Catal. B* **2009**, *88*, 413–419.

42. Ravel, B.; Newville, M. ATHENA, ARTEMIS, HEPHAESTUS: data analysis for X-ray absorption spectroscopy using IFEFFIT. *J. Synchrotron Radiat.* **2005**, *12*, 537–541.